

OPEN

Antigen sampling by intestinal M cells is the principal pathway initiating mucosal IgA production to commensal enteric bacteria

D Rios¹, MB Wood¹, J Li¹, B Chassaing², AT Gewirtz² and IR Williams¹

Secretory IgA (SIgA) directed against gut resident bacteria enables the mammalian mucosal immune system to establish homeostasis with the commensal gut microbiota after weaning. Germinal centers (GCs) in Peyer's patches (PPs) are the principal inductive sites where naive B cells specific for bacterial antigens encounter their cognate antigens and receive T-cell help driving their differentiation into IgA-producing plasma cells. We investigated the role of antigen sampling by intestinal M cells in initiating the SIgA response to gut bacteria by developing mice in which receptor activator of nuclear factor- κ B ligand (RANKL)-dependent M-cell differentiation was abrogated by conditional deletion of *Tnfrsf11a* in the intestinal epithelium. Mice without intestinal M cells had profound delays in PP GC maturation and emergence of lamina propria IgA plasma cells, resulting in diminished levels of fecal SIgA that persisted into adulthood. We conclude that M-cell-mediated sampling of commensal bacteria is a required initial step for the efficient induction of intestinal SIgA.

INTRODUCTION

IgA antibodies have a major role in maintaining homeostasis at mucosal surfaces including the gastrointestinal tract.^{1,2} Peyer's patches (PPs) are critical inductive sites in the mammalian small intestine where naive B cells are initially activated by exogenous luminal antigens and then differentiate with T-cell help into IgA plasmablasts that circulate in the blood before preferentially homing to the intestinal lamina propria to become resident IgA-secreting plasma cells.^{3,4} High local concentrations of transforming growth factor- β and retinoic acid, and the presence of interleukin-21-producing follicular helper T cells are all factors that promote IgA class switching in PPs.^{5,6} Many of the dimeric IgA antibodies produced by lamina propria IgA-secreting plasma cells are transcytosed across the epithelial layer and bind to commensal enteric bacteria after reaching the lumen.⁷ Secretory IgA (SIgA) directed against bacterial antigens has a variety of effects that help to shape gut microbial populations including immune exclusion from the inner mucus layer, inhibition of bacterial motility, impairment of bacterial fitness and neutralization of toxins.^{2,8,9} Commensal bacteria resident in the small intestine are more efficient than those in the cecum and colon at eliciting a robust host SIgA response that leads to

coating of the bacteria with SIgA detectable by bacterial flow cytometry. The increased SIgA coating of small intestinal bacteria by SIgA correlates with enhanced priming of B cells to bacterial antigens in the small intestinal gut-associated lymphoid tissue (GALT).¹⁰ In addition, high levels of bound IgA on gut resident bacteria may flag those commensal bacteria with a propensity to elicit a strong host immune response and induce colitis, leading to intestinal pathology.¹¹ The meager SIgA response of germ-free mice supports the concept that the commensal microbiota is the major stimulus that elicits the normal homeostatic SIgA response.^{12,13}

Several distinct antigen-sampling mechanisms are used to transport luminal antigens across the intestinal epithelium to initiate an adaptive immune response.¹⁴ Antigen-sampling cells include M cells found in the follicle-associated epithelium overlying PPs and isolated lymphoid follicles,¹⁵ macrophages and dendritic cells that directly sample luminal antigens by sending transepithelial dendrites between or through epithelial cells^{16–18} and goblet cells that can provide a conduit for low-molecular-weight antigens to traverse the epithelial layer and reach mononuclear phagocytes in the lamina propria.¹⁹ However, the relative contributions of these various

¹Department of Pathology and Laboratory Medicine, Emory University School of Medicine, Atlanta, Georgia, USA and ²Center for Inflammation, Immunity and Infection, Institute for Biomedical Sciences, Georgia State University, Atlanta, Georgia, USA. Correspondence: IR Williams (irwilli@emory.edu)

Received 22 April 2015; accepted 8 October 2015; published online 25 November 2015. doi:10.1038/mi.2015.121

antigen-sampling pathways to the SIgA response to antigens from commensal bacteria are not known.

M cells are specialized phagocytic epithelial cells with several adaptations that facilitate their ability to efficiently sample particulate antigens. Blunted microvilli and an attenuated glycocalyx allow antigens to come in close proximity to the apical surface of M cells, whereas a basolateral invagination allows for positioning of antigen-presenting cells (APCs) and lymphocytes in very close proximity to the lumen.²⁰ M cell antigen sampling can occur either through clathrin-coated endocytic vesicles²¹ for larger antigens or via fluid phase pinocytosis for smaller antigens.^{22,23} Antigens acquired by M cells through their apical surface are rapidly shuttled via vesicular transport to the basolateral membrane where they are released, enabling uptake by APCs and processing for presentation to T cells and transport to follicular dendritic cells present within the B-cell follicles. Differentiation of M cells from uncommitted precursors in intestinal crypts is dependent on receptor activator of nuclear factor- κ B ligand (RANKL)-expressing subepithelial stromal cells that are normally restricted to organized lymphoid structures such as PPs and isolated lymphoid follicles.^{24,25}

We previously showed that intestinal M cells are absent in PPs from RANKL-deficient mice.²⁵ However, the critical involvement of RANKL–RANK signaling in multiple facets of immune system development including lymph node formation²⁶ and medullary thymic epithelial cell differentiation²⁷ detracts from the value of global RANKL or RANK knockout mice as models to investigate how loss of intestinal M cells perturbs mucosal immune responses. To restrict the effects of interrupting the RANKL–RANK signaling axis to the intestinal epithelium, we generated a conditional knockout mouse in which *Tnfrsf11a* (the gene encoding RANK) is only deleted in intestinal epithelial cells. These RANK ^{Δ IEC} mice represent a first-of-its-kind model system in which intestinal M-cell-mediated antigen uptake is ablated, whereas other RANKL–RANK-dependent developmental events required for normal immune system function are not impacted. Our analysis of the SIgA response in the intestine of RANK ^{Δ IEC} mice demonstrates the pivotal role M cells have in facilitating sampling of the commensal microbiota by GALT, which initiates SIgA production and is, in turn, key to the maintenance of homeostasis in epithelial tissues richly colonized by the commensal microbiota.

RESULTS

Conditional deletion of RANK in the intestinal epithelium results in the absence of PP M cells

A villin-cre transgene was bred to mice homozygous for a floxed allele of RANK (RANK^{F/F}), to generate mice lacking RANK expression in the intestinal epithelium (designated RANK ^{Δ IEC}) (Supplementary Figure S1 online). Whole mounts and cross-sections of intestinal PPs from adult RANK^{F/F} and RANK ^{Δ IEC} mice were stained with anti-GP2 antibody to detect M cells (Figure 1a–d). The PP domes of RANK^{F/F} mice typically contained 150–200 GP2-expressing M cells. In contrast, no GP2⁺ cells were detected in RANK ^{Δ IEC} mice. Absorptive

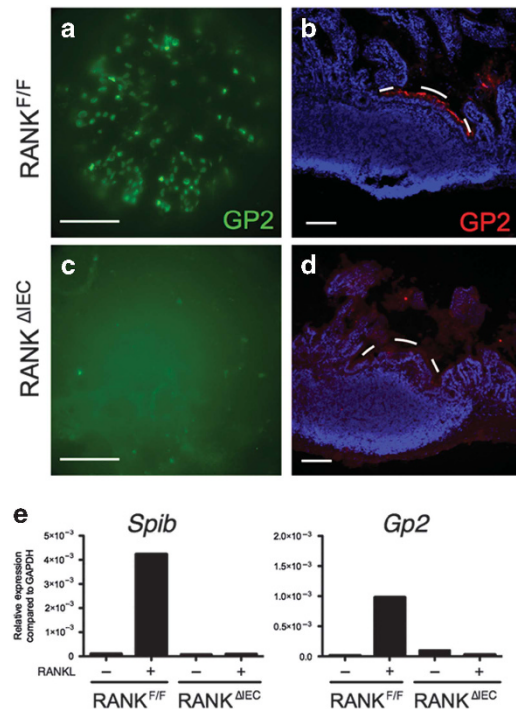


Figure 1 RANK ^{Δ IEC} mice lack Peyer's patch (PP) M cells. Representative images showing the distribution of GP2⁺ M cells in PPs from RANK^{F/F} and RANK ^{Δ IEC} mice as observed on whole mounts (a,c) and cryosections (b,d). The white dashes in b and d form an arc just above the apical surface of the follicle-associated epithelium (FAE). Bar = 100 μ m. (e) Enteroid cultures of crypt cells from RANK^{F/F} and RANK ^{Δ IEC} mice were cultured for 3 days in the presence or absence of RANKL. The level of expression of M-cell-associated genes *Spib* and *Gp2* was determined by quantitative PCR and the results normalized to *Gapdh*. Data are representative of three experiments done with independently derived enteroid cultures. See also Supplementary Figure 1 for additional information on the floxed RANK allele and Supplementary Figure 2 for a histologic comparison of goblet cell and Paneth cell differentiation in RANK^{F/F} and RANK ^{Δ IEC} mice.

enterocytes, goblet cells, and Paneth cells differentiated normally in the small intestine of RANK ^{Δ IEC} mice (Supplementary Figure S2). To further evaluate the penetrance of the intestinal M-cell differentiation defect in RANK ^{Δ IEC} mice, we used an *in vitro* model of RANKL-stimulated M-cell differentiation in enteroid cultures similar to that described by de Lau *et al.*²⁸ Addition of RANKL to enteroid cultures established from RANK^{F/F} mice led to robust induction of M-cell-specific genes including *Spib* and *Gp2* after 3 days compared with unstimulated cultures (Figure 1e). In contrast, RANKL was unable to induce M-cell-specific genes in enteroids from RANK ^{Δ IEC} mice. Thus, the villin-cre transgene-mediated deletion of the *Tnfrsf11a* gene encoding RANK was fully penetrant in uncommitted crypt enterocytes and completely abrogated differentiation of the M-cell lineage.

Peps in RANK ^{Δ IEC} mice are deficient in uptake of particulate antigens

To assess the impact of the absence of M cells in RANK ^{Δ IEC} mice on uptake of particulate antigens from the intestinal lumen, RANK ^{Δ IEC} and RANK^{F/F} mice were gavage-fed

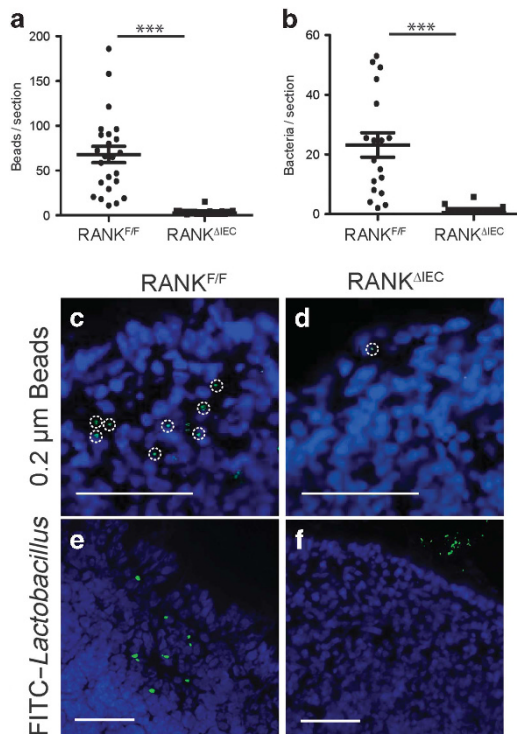


Figure 2 Peyer's patches (PPs) lacking M cells have reduced capacity to phagocytose particulate antigens. $RANK^{F/F}$ and $RANK^{\Delta IEC}$ mice were gavaged fed with either 1×10^{11} 0.2- μ m diameter fluorescein isothiocyanate (FITC)-labeled polystyrene beads (a) or 1×10^9 colony-forming unit (CFU) FITC-labeled *L. rhamnosus* strain GG (LGG) (b), followed by excision of the PPs after 6 h (a) or 24 h (b). Individual points on the scatter plots represent the number of beads or bacteria manually counted in cryosections of a single PP follicle (a) or the entire PP (b). (c,d) Representative images showing 0.2- μ m diameter beads within PPs from $RANK^{F/F}$ (c) and $RANK^{\Delta IEC}$ (d) mice. The dashed circles show individual phagocytic cells containing multiple beads. (e,f) Representative images showing FITC-LGG within PPs from $RANK^{F/F}$ (e) and $RANK^{\Delta IEC}$ (f) mice. Bar = 100 μ m. Data from each group are summarized as mean \pm s.e.m. and are representative of two experiments with three mice per group. *** $P < 0.001$ (t-test).

particulate antigens known to be taken up into PPs via M cells. The uptake of fluorescent 0.2 μ m polystyrene beads or fluorescently labeled *Lactobacillus rhamnosus* strain GG (LGG) bacteria was measured by counting the number of beads or bacteria observed in sections of the PP dome (Figure 2). Numerous 0.2 μ m polystyrene beads were detected within the PPs of $RANK^{F/F}$ mice 24 h after gavage (Figure 2a,c). In $RANK^{\Delta IEC}$ mice, uptake of polystyrene beads into PPs was reduced by over 90%, although not completely eliminated (Figure 2a,d). We speculate that the low level of residual sampling of polystyrene beads in $RANK^{\Delta IEC}$ mice is mediated by one or more of the M-cell-independent antigen uptake pathways. Examination of the uptake of fluorescein isothiocyanate (FITC)-labeled LGG bacteria 6 h after gavage revealed a more pronounced uptake deficit in the $RANK^{\Delta IEC}$ mice (with $< 1\%$ of the uptake in $RANK^{F/F}$ mice), with the vast majority of sections examined showing no bacterial uptake at all (Figure 2b,e,f). The substantially larger size of the LGG bacteria compared with the 0.2 μ m beads is likely responsible for the greater dependence on M cells for bacterial uptake into PPs.

Germinal center development is delayed in the PP follicles of $RANK^{\Delta IEC}$ mice

In wild-type adult mice, all PP follicles contain active germinal centers (GCs), with GC development occurring rapidly after mice are weaned from their mothers.²⁹ To determine whether loss of M cells and M-cell-mediated particulate antigen uptake affected the maturation of PP follicles, we compared the size of PP follicles in $RANK^{F/F}$ and $RANK^{\Delta IEC}$ mice at 1 and 3 weeks after weaning by measuring the follicular area in sections. $RANK^{\Delta IEC}$ mice showed a significant reduction in the size of the B-cell follicles at 1 week after weaning (Supplementary Figure 3). Follicle size increased between 1 and 3 weeks after weaning in both groups, with the follicles remaining smaller in $RANK^{\Delta IEC}$ mice compared with $RANK^{F/F}$ littermates. To directly assess the formation of GCs within these follicles, we stained PP sections with anti-GL7, a marker of GC B cells, and anti-IgD to define the borders of the GCs (Figure 3a–d). In PP follicles from $RANK^{F/F}$ mice, a few IgD⁺ cells in the center of the follicle were already GL7⁺ at 1 week after weaning and by 3 weeks after weaning almost all follicles had easily appreciated clusters of GL7⁺ cells within the IgD⁺ GC area. In contrast, only a minority of the PP follicles in $RANK^{\Delta IEC}$ mice had clusters of GL7⁺ cells within the IgD⁺ area of the follicle at 3 weeks after weaning. Analysis of PP cell suspensions by flow cytometry confirmed that fewer CD19⁺ IgD⁺ GL7^{hi} GC B cells and CD4⁺ PD-1^{hi} CXCR5⁺ follicular helper T cells are present in the PPs of $RANK^{\Delta IEC}$ mice at 2 weeks after weaning (Figure 3e,f and Supplementary Figure 3). By 6 weeks after weaning, the density of GL7⁺ GC B cells and CD21/35⁺ follicular dendritic cells was comparable in $RANK^{\Delta IEC}$ and $RANK^{F/F}$ mice (Supplementary Figure 4). Thus, GC formation in PP follicles is delayed in $RANK^{\Delta IEC}$ mice lacking M cells.

The density of lamina propria IgA-secreting plasma cells and the concentration of fecal IgA are reduced in $RANK^{\Delta IEC}$ mice

GCs in PP follicles are known to be major inductive sites where B-cells class switch to IgA and differentiate into IgA-secreting plasma cells that home to the intestinal lamina propria. We investigated whether the impaired antigen uptake into PPs of $RANK^{\Delta IEC}$ mice was associated with a deficiency in cells producing SIgA (Figure 4). By 1 week after weaning, groups of IgA⁺ antibody-secreting cells (ASCs) were present at the base of small intestinal villi in $RANK^{F/F}$ mice; at 4 weeks after weaning, a high density of IgA⁺ ASCs was found throughout the villi (Figure 4a,b). In contrast, only rare scattered IgA⁺ ASCs were present in the lamina propria of $RANK^{\Delta IEC}$ mice 1 week after weaning (Figure 4c). By 4 weeks after weaning, the density of IgA⁺ ASCs in $RANK^{\Delta IEC}$ mice had increased (Figure 4d), but remained lower than that observed in $RANK^{F/F}$ littermates (Figure 4b). Flow cytometry of small intestine lamina propria cell suspensions was performed at 1 and 4 weeks after weaning, to quantify the extent of IgA plasma cell differentiation (Figure 4e and Supplementary Figure 5). Very few IgA⁺ CD138⁺ plasma cells were detected in $RANK^{\Delta IEC}$ mice at 1 week after weaning. At 4 weeks after weaning, a population of

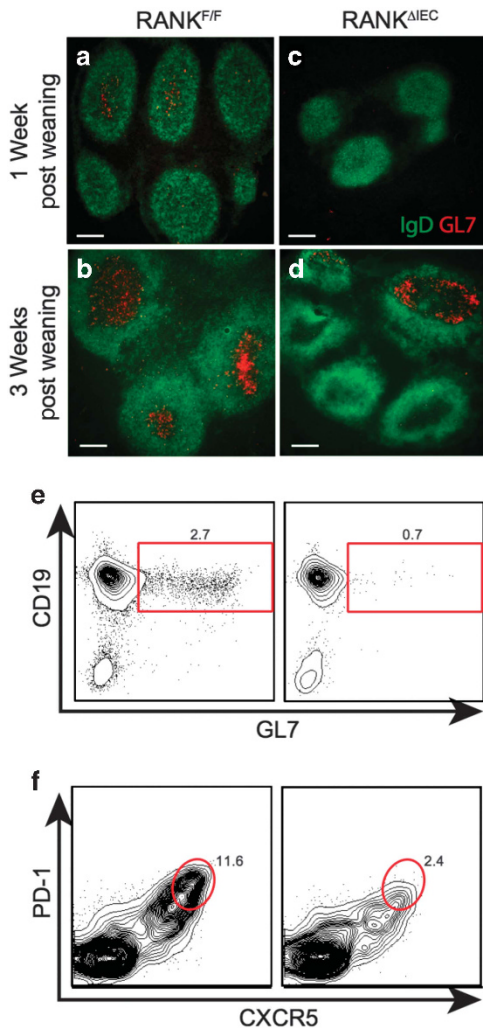


Figure 3 Germinal center (GC) formation is delayed in Peyer's patches (PPs) lacking M cells. Representative images of horizontal sections of PPs from $RANK^{F/F}$ and $RANK^{\Delta IEC}$ mice at 1 week (**a,c**) and 3 weeks (**b,d**) after weaning, showing the density of $GL7^+$ GC B cells within the IgD^- region of follicles. Bars = 100 μ M. (**e,f**) Representative flow plots of PP lymphocytes from $RANK^{F/F}$ and $RANK^{\Delta IEC}$ mice at 2 weeks after weaning, stained for CD19 and GL7 to detect GC B cells (**e**) or PD-1 and CXCR5 to detect follicular helper T (Tfh) cells (**f**). Cells analyzed were gated on live $CD45^+$ singlets that were also $B220^+$ (**e**) or $CD4^+$ (**f**). Data are representative of two experiments with three mice per group. See also **Supplementary Figures 3 and 4**.

IgA^+ $CD138^+$ cells was present in $RANK^{\Delta IEC}$ mice but the frequency of these cells remained less than that in $RANK^{F/F}$ littermates. There were no significant differences in frequencies of IgA^+ plasma cells at any time points in the mesenteric lymph node or spleen (**Supplementary Figure 5**). As most of the IgA produced by IgA^+ ASCs in the intestinal lamina propria is transcytosed across the epithelium and released into the lumen as SIgA, we also compared the concentration of fecal IgA in control and mutant mice at multiple time points beginning 4 days before weaning (**Figure 5a**). As neonatal mice transition from mother's milk to mouse chow as their primary food source, the concentration of fecal IgA drops to a nadir reached around 1 day after weaning. Tracking the production of fecal IgA at daily

time points revealed that by 4 days post weaning there was a significant increase above baseline in fecal IgA production in all $RANK^{F/F}$ mice (**Figure 5b**). In contrast, there was not a significant uptick in fecal IgA production in any $RANK^{\Delta IEC}$ mice until at least 7 days after weaning. In M-cell-deficient $RANK^{\Delta IEC}$ mice, fecal IgA levels were lower throughout the first 5 weeks after weaning compared with $RANK^{F/F}$ littermates (**Figure 5a**). Although fecal IgA levels did progressively increase in $RANK^{\Delta IEC}$ mice, the rate of this increase and the plateau concentration of fecal IgA reached in adults were significantly decreased compared with $RANK^{F/F}$ controls (**Figure 5c**). Although most of the IgA produced in the intestinal lamina propria ends up as SIgA, we also investigated whether serum IgA levels were affected in $RANK^{\Delta IEC}$ mice. $RANK^{\Delta IEC}$ mice also had significantly lower serum IgA levels than $RANK^{F/F}$ mice at 1 week after weaning but this difference was no longer apparent by 3 weeks after weaning (**Supplementary Figure 6**). The concentrations of serum IgM and IgG were equivalent in both genotypes at all time points tested.

$RANK^{\Delta IEC}$ mice display an impaired SIgA response to oral immunization with a protein antigen

To determine whether the absence of intestinal M cells in $RANK^{\Delta IEC}$ mice diminished their capacity to mount an antigen-specific SIgA response following oral exposure to a foreign protein antigen, 5-week-old $RANK^{\Delta IEC}$ and $RANK^{F/F}$ littermates were immunized with horse spleen ferritin.³⁰ Ferritin was added to their drinking water on days 0–2 and then again on days 7–9. Two weeks after the initial immunization, a ferritin-specific fecal IgA response was readily detected in $RANK^{F/F}$ mice but anti-ferritin IgA levels in $RANK^{F/F}$ littermates were still comparable to unimmunized controls (**Supplementary Figure 7**).

Enteric bacteria in fecal samples from $RANK^{\Delta IEC}$ mice have less bound SIgA

A significant portion of the normal SIgA repertoire in the intestine is directed against antigens found on enteric bacteria.⁷ We prepared suspensions of fecal bacteria from $RANK^{\Delta IEC}$, $RANK^{F/F}$, and $JH^{-/-}$ mice, and measured the amount of IgA bound to individual bacteria by flow cytometry with a labeled secondary anti- IgA monoclonal antibody (**Figure 6**). As expected, bound IgA was not detected on fecal bacteria from $JH^{-/-}$ mice (data not shown). At 4 weeks after weaning, the fraction of fecal bacteria coated by IgA and the average amount of bound IgA per bacterium were both decreased in $RANK^{\Delta IEC}$ samples compared with $RANK^{F/F}$ controls.

Effect of delayed and decreased SIgA production by $RANK^{\Delta IEC}$ mice on composition of the fecal microbiota

As production of SIgA is one of the pivotal host immune responses involved in establishing homeostasis with the gut microbiota, we investigated whether the absence of M cells and the associated SIgA deficit in $RANK^{\Delta IEC}$ mice resulted in perturbations in the composition of the gut microbiota. Fecal samples from co-housed littermate $RANK^{\Delta IEC}$ and $RANK^{F/F}$ mice were collected at 3, 7, 20, 30, and 40 days after weaning. Illumina (San Diego, CA) sequencing of 16S rRNA amplicons

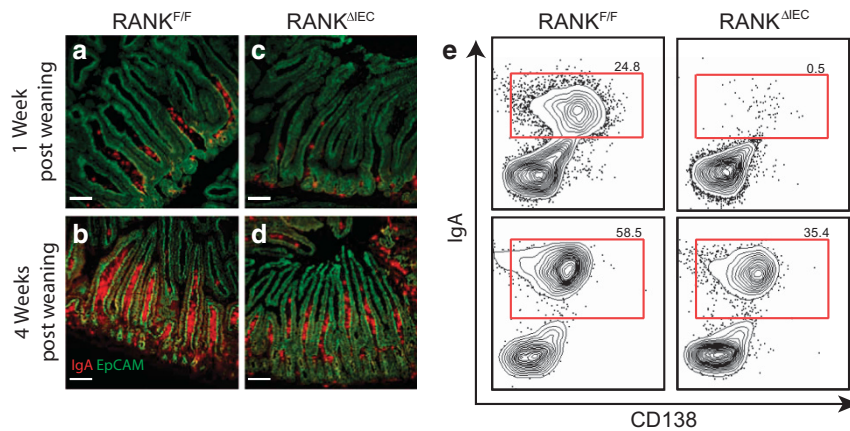


Figure 4 Frequency of lamina propria IgA⁺ plasma cells is reduced in RANK^{ΔIEC} mice. Representative cryosections of small intestine from RANK^{F/F} (a,b) or RANK^{ΔIEC} mice (c,d) at 1 week (a,c) or 4 weeks (b,d) after weaning were stained with anti-EpCAM (green) and anti-IgA (red). Bars = 100 μM. (e) Representative flow plots from cells isolated from small intestinal lamina propria at 1 and 4 weeks after weaning. Cells analyzed were gated on live CD45⁺ singlets that were also B220⁻ and IgD⁻. Data are representative of two experiments with three mice per group. See also **Supplementary Figure 5**.

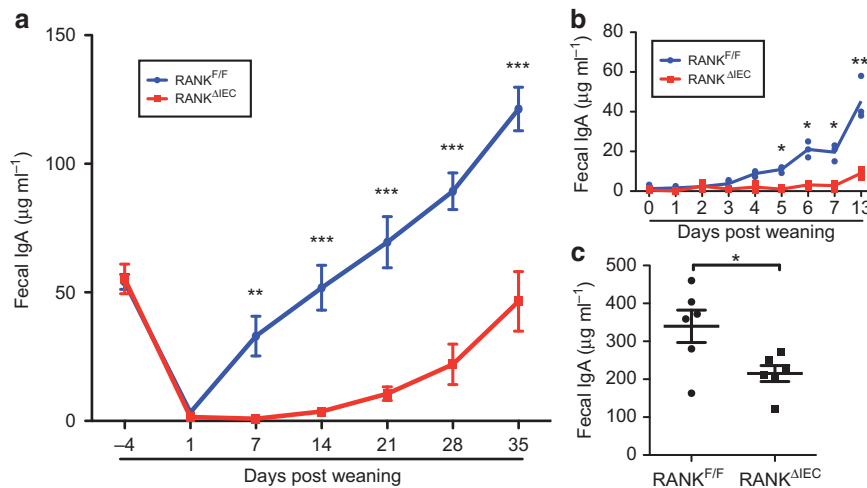


Figure 5 Production of fecal IgA is delayed and reduced in RANK^{ΔIEC} mice. (a) Fecal IgA concentrations of RANK^{F/F} and RANK^{ΔIEC} mice were determined at multiple time points starting at 4 days before weaning. Data are summarized as mean \pm s.e.m. and are representative of four experiments with four mice of each genotype. (b) Fecal IgA concentrations of RANK^{F/F} and RANK^{ΔIEC} mice at daily time points beginning at weaning. Data are representative of two experiments with three mice of each genotype. (c) Fecal IgA concentrations in adult mice 8–10 weeks after weaning. Data are summarized as mean \pm s.e.m. and are from a single experiment with six mice of each genotype. * $P < 0.05$, ** $P < 0.01$ (*t*-test). See also **Supplementary Figure 6**.

revealed no substantive shifts at the family level in the types of bacteria present in the two genotypes of mice and a comparable amount of alpha diversity (**Supplementary Figure 8**).

Impaired induction of SIgA after conventionalization of germ-free RANK^{ΔIEC} mice

SIgA responses in the intestine of germ-free mice are markedly suppressed due to the absence of the microbiota that normally provides the dominant source of antigens eliciting this response.^{31,32} Conventionalization of previously germ-free mice normally results in a rapid rebound of the SIgA response.³ To examine the impact of loss of intestinal M cells on fecal IgA responses in the germ-free condition and after

conventionalization, we established a germ-free colony of RANK^{ΔIEC} mice housed with RANK^{F/F} littermates. Both groups produced equally low concentrations of fecal IgA after weaning and the IgA concentrations rose slightly to reach a plateau around 4 weeks after weaning that was far below the typical fecal IgA concentration detected in conventionally housed mice (**Figure 7a**). When groups of germ-free RANK^{ΔIEC} mice and RANK^{F/F} controls were acutely conventionalized at the time of weaning with the microbiota present in the specific pathogen-free mouse colony, the M-cell-deficient mice exhibited significantly decreased fecal IgA responses at 4 and 6 weeks after weaning (**Figure 7b**). This deficit in fecal IgA production recapitulated the fecal IgA phenotype observed in

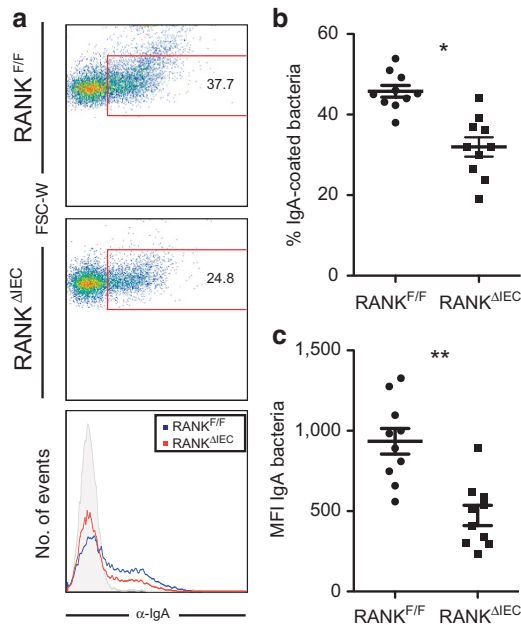


Figure 6 *In vivo* IgA coating of commensal microbiota is decreased in $RANK^{\Delta IEC}$ mice. **(a)** Representative flow plots of fecal bacteria isolated from $RANK^{F/F}$ and $RANK^{\Delta IEC}$ mice 4 weeks after weaning and stained with anti-IgA. **(b,c)** The percentage of IgA⁺ fecal bacteria **(b)** and the mean fluorescence intensity of IgA binding **(c)** were determined using fecal bacteria from $RANK^{F/F}$ and $RANK^{\Delta IEC}$ mice. Data are summarized as mean \pm s.e.m. and are from 1 experiment with 10 mice per group. * $P < 0.05$, ** $P < 0.01$ (*t*-test).

the original specific pathogen-free colony (**Supplementary Figure 5**) and confirmed that the absence of antigen-sampling M cells is sufficient to seriously compromise the rapid host SIgA response elicited by conventionalization of germ-free mice.

DISCUSSION

One of the cardinal features of mucosal immunity in mammals is the synthesis and transepithelial transport of large amounts of SIgA that contribute to maintaining homeostasis with the enteric microbiota.^{4,33} Endogenous SIgA production normally begins shortly after weaning, coincident with a shift from breast milk to solid food as the main nutrition source and accelerated colonization of the intestine by commensal bacteria. The initial endogenous SIgA response is dominated by IgA antibodies with few, if any, mutations in their variable regions and low avidity for the bacteria in the lumen.³⁴ As the mucosal immune system matures, most of the SIgA antibodies secreted in the intestine carry mutations concentrated in the complementarity-determining regions of VH and VL domains. These mutations occur as a result of T-cell-dependent somatic mutation in GCs and lead to increased avidity of the antibodies for target antigens. B-cell clones responding to foreign antigens that persist can undergo additional rounds of somatic mutation in GALT GCs contributing to further increases in antibody affinity.³⁵

A major source of antigens driving SIgA production in the intestine is the commensal enteric flora. As a result, germ-free mice have a markedly attenuated SIgA response.^{31,36} Furthermore, SIgA production in germ-free mice can be restored to

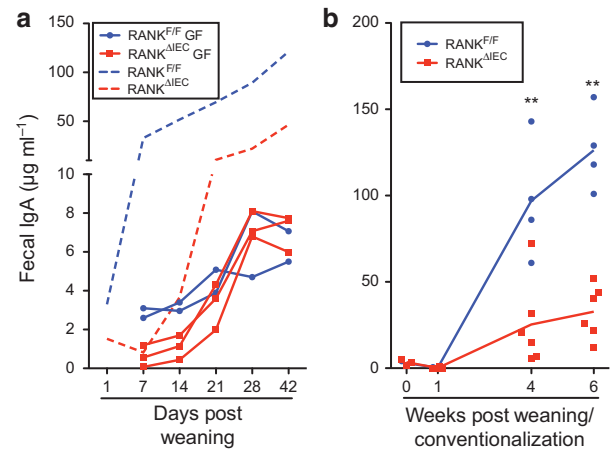


Figure 7 M cells are required to initiate IgA responses to the intestinal microbiota. **(a)** The solid lines show fecal IgA concentrations in individual $RANK^{F/F}$ and $RANK^{\Delta IEC}$ littermates housed in a germ-free isolator from birth through 9 weeks of age. Data are from one of two litters that yielded similar results. The dashed lines show for comparison purposes the mean fecal IgA concentrations for $RANK^{F/F}$ and $RANK^{\Delta IEC}$ littermates housed under standard specific pathogen-free (SPF) conditions (data from **Figure 5**). **(b)** A single germ-free litter consisting of four $RANK^{F/F}$ mice and six $RANK^{\Delta IEC}$ mice was conventionalized by exposure to SPF fecal microbiota at weaning. The concentration of fecal IgA was determined at weaning and several time points after weaning. ** $P < 0.01$ (unpaired *t*-test). See also **Supplementary Figure 9**.

near normal levels over the course of several weeks after conventionalization with bacterial species that can establish stable residence in the intestine.³ For the host immune system to mount an IgA response to antigens originating with the commensal microbiota, bacterial antigens must cross the epithelium and reach APCs that display the antigens enabling stimulation and expansion of reactive B cells and T cells. This antigen sampling process can potentially involve either soluble antigens or whole bacteria. The relative contributions to the overall SIgA response of the main cellular pathways that participate in *in vivo* sampling of antigens from the intestinal lumen (i.e., M cells, mononuclear phagocytes, and goblet cells) have not been established.¹⁴ A series of technical limitations have made it impractical or impossible to selectively eliminate just one of these antigen sampling pathways *in vivo* in the intestine. For example, mice lacking any intestinal goblet cells die shortly after weaning due to severe problems with establishment of the normal mucus barrier.³⁷ Although some knockout mouse strains either lack or have induced defects in specific DC and macrophage subsets, there is not yet an established model with a complete absence of all mononuclear phagocyte subsets. The absence of suitable mouse models featuring complete abrogation of individual intestinal antigen sampling pathways has hampered efforts to assess the individual contributions of each cellular pathway.

We sought to develop mice with selective absence of intestinal M cells by drawing mice on previous work that established the dependence of intestinal M-cell differentiation on RANKL–RANK signaling.²⁵ Cre-mediated deletion of a floxed *Tnfrsf11a* gene restricted to enterocytes yielded mice in which

RANKL-directed differentiation of intestinal M cells from uncommitted precursors in follicle-associated crypts did not occur. The functional consequence of the absence of M cells in these 'M-less' mice was a profound deficit in the uptake of several types of model particulate antigens (0.2 μ m beads and bacteria) into PPs, confirming that M cells are responsible for the vast majority of uptake of these classes of antigens into GALT structures. The other major cell types responsible for intestinal antigen sampling (mononuclear phagocytes and goblet cells) remain functionally intact in these mice, which enabled us to investigate whether loss of the M-cell antigen-sampling pathway alone interfered with specific types of mucosal immune responses.

Seminal work by Craig and Cebra³⁸ identified PPs as a rich source of lymphocyte precursors capable of differentiating into IgA-secreting plasma cells in the intestinal lamina propria after adoptive transfer. Although M-cell-mediated antigen sampling is restricted to GALT structures such as PPs, the other major antigen sampling mechanisms described in the intestine are also functional in GALT structures and could therefore contribute to inducing IgA responses at these sites. The substantial deficit in the post-weaning SIgA response observed in the RANK ^{Δ IEC} mouse model proves that antigen sampling by GALT M cells is pivotal for the efficient early generation of IgA responses. A closely correlated feature of the deficient inductive environment in PPs from RANK ^{Δ IEC} mice was delayed appearance of recognizable GCs within the B-cell follicles. The decreased amount of total fecal IgA secreted into the intestinal lumen of RANK ^{Δ IEC} mice also correlated well with flow cytometry results showing a decreased amount of IgA bound to fecal bacteria. RANK ^{Δ IEC} mice also displayed a defect in the induction of fecal IgA responses to a newly introduced oral protein antigen, confirming that lack of intestinal M cells results in a generalized defect in the rapid induction of IgA responses to foreign antigens encountered in the gut lumen.

When the normal commensal microbiota was eliminated as a potential source of antigens inducing the SIgA response by studying germ-free RANK ^{Δ IEC} mice, the weak residual SIgA response was not significantly different from that of the control RANK^{F/F} littermates. Thus, the normal SIgA response of mice that briskly develops following weaning depends on sampling of the commensal microbiota by M cells. The availability of this efficient M-cell-mediated antigen-sampling pathway is one of the major factors responsible for the high frequency of precursors to mature IgA-secreting plasma cells in PPs compared with the blood and peripheral lymph nodes.³⁸

We also found that the extent of the fecal IgA deficit observed in RANK ^{Δ IEC} mice compared with RANK^{F/F} controls was partially attenuated as the mice progressed toward adulthood. Several factors likely contribute to this narrowing of the difference between the two genotypes over time. As antigen sampling is not impaired at the non-intestinal mucosal sites in RANK ^{Δ IEC} mice, normal initiation of IgA responses occurs at these other mucosal sites. Not all IgA plasma cells induced within a single mucosal tissue end up homing back to effector sites in the same mucosal tissue. The partial overlap in the

homing mechanisms used for IgA plasma cells to return to the various mucosal tissues allows some IgA plasma cells induced in non-intestinal mucosal tissues to end up localizing to the intestine.^{1,39,40} Another factor in narrowing the gap between the two genotypes is further expansion of the initial clones of memory B cells and plasma cells that reach the intestine. As IgA-producing B cells can re-enter GCs to proliferate further and undergo receptor diversification,³⁵ we speculate that the few IgA-secreting plasma cells that initially seed the lamina propria of RANK ^{Δ IEC} mice have the potential to be amplified in PPs, leading to increases in the number of lamina propria plasma cells and the amount of SIgA even if the diversity of the resulting IgA repertoire remains substantially constricted compared with wild-type mice as a consequence of decreased transport of commensal microbiota antigens into the inductive sites via M cells. Finally, some of the SIgA normally present in feces initially enters the gastrointestinal tract as a constituent of bile. Hepatocytes and biliary epithelial cells expressing the polymeric immunoglobulin receptor can transcytose dimeric IgA and deliver this SIgA into the gut lumen to add to the IgA transcytosed across the intestinal epithelium by enterocytes.⁴¹

Our findings support a fundamental role for M cells in driving SIgA responses that are targeted toward commensal bacteria. Despite the scarcity of M cells relative to other cell types in the intestinal epithelium and underlying lamina propria, M cells have a critical and non-redundant role in establishment of normal secretory immunity at inductive GALT sites.

METHODS

Conditional RANK knockout mice. Mice with a conditional allele of *Tnfrsf11a* (the gene encoding RANK) featuring loxP sites flanking exons 2 and 3 were produced at inGenious Targeting Laboratory (Stony Brook, NY). Mice carrying this floxed allele were donated to The Jackson Laboratory Mouse Repository (<http://jaxmice.jax.org/strain/027495.html>); the official strain designation is B6.Cg-Tnfrsf11a^{tm1.11rw}/J. Mice with the floxed allele were bred to villin-cre mice (Tg(Vil-cre)997Gum/J strain; The Jackson Laboratory, Bar Harbor, ME), to produce mice homozygous for the floxed RANK allele that also carried the villin-cre transgene (villin-cre RANK^{F/F} genotype; also designated RANK ^{Δ IEC} and referred to as 'M-less'). Most experimental mice used in experiments originated from breeding pairs of male RANK ^{Δ IEC} mice and female RANK^{F/F}, and consisted of a mix of RANK ^{Δ IEC} mice and RANK^{F/F} littermates used as controls. Litters were weaned at 21 days after birth. All animal studies were reviewed and approved by the Emory University Institutional Animal Care and Use Committee.

Germ-free conditional RANK knockout mice. Germ-free rederivation of the RANK ^{Δ IEC} mouse strain was done at Taconic (Germantown, NY). Rederived mice confirmed to be germ-free at Taconic were shipped to the germ-free mouse facility at Georgia State University, to establish a breeding colony. The germ-free status of the isolators used for these studies was verified on a regular basis by quantitative PCR with primers for 16S rDNA sequences. For conventionalization experiments, germ-free mice were transferred from isolators to conventional housing and initially exposed to drinking water containing fecal bacteria from conventionally housed specific pathogen-free mice in the same mouse facility. The studies done in this facility using germ-free and gnotobiotic RANK ^{Δ IEC} and RANK^{F/F} mice were reviewed and approved by the Georgia State Institutional Animal Care and Use Committee.

Immunofluorescence staining of M cells. For whole mount preparations, PPs were isolated directly into cold Dulbecco's modified Eagle's media and then incubated for 10 min at room temperature in 1% *N*-acetyl cysteine followed by vigorous vortexing to dissociate the mucus layer. The PPs were fixed in 4% paraformaldehyde for 30 min at 20 °C. For frozen section preparations, PPs were cut transversely through the dome area, embedded in optimal cutting temperature compound, and sectioned with a cryostat as previously described.²⁴ Both whole mounts and cryosections were incubated overnight at 4 °C with anti-GP2 antibody (2F11-C3; MBL, Woburn, MA) and rhodamine-UEA-I (Vector Labs, Burlingame, CA) in TBB buffer (PerkinElmer, Waltham, MA) containing 0.25% saponin. The whole mounts and sections were washed for 10 min with TBB with 0.25% saponin and incubated with Alexa647-conjugated polyclonal goat anti-rat antibody (Invitrogen, Grand Island, NY) for 3 h at 20 °C. DAPI (4',6-diamidino-2-phenylindole; Sigma-Aldrich, St. Louis, MO) was added to the frozen sections as a nuclear counterstain. Whole mounts and frozen sections were mounted in ProLong Gold antifade reagent (Invitrogen) and held for 1 h at 4 °C in the dark before image acquisition using a Nikon (Melville, NY) 80i epifluorescence microscope.

Immunofluorescence staining of GCs and IgA-secreting cells. For analysis of PP GCs, horizontal sections of PPs were stained overnight at 4 °C with FITC- or phycoerythrin (PE)-conjugated anti-IgD (11-26c; eBioscience, San Diego, CA), allophycocyanin (APC)-conjugated anti-GL7 (GL-7; eBioscience), and FITC-conjugated anti-CD21/35 (7G6; BD Biosciences, San Jose, CA). Lamina propria IgA-secreting cells were detected with FITC-conjugated anti-IgA (C10-3; BD Biosciences) and the location of the epithelium was defined using APC-conjugated anti-EpCAM (G8.8; eBioscience).

Enteroid cultures for *in vitro* induction of M-cell differentiation. Small intestinal crypts from the distal 10 cm of the small intestine were isolated and cultured in Matrigel (Corning, Tewksbury, MA) to generate three-dimensional enteroids using a modified version of published methods.^{42,43} After 3 days of culture, the media above the Matrigel was replaced and half the wells were supplemented with 100 ng ml⁻¹ of soluble mouse RANKL (Peprotech, Rocky Hill, NJ) for 3 days to induce M-cell differentiation.

Quantitative real-time PCR analysis of gene expression in enteroids. The Matrigel droplet containing enteroids was incubated with 500 µl of Cell Recovery Solution (Corning) for 1 h at 4 °C. Once the Matrigel was depolymerized, the cell pellet was washed and used for extraction of RNA. cDNA was synthesized with the iScript cDNA synthesis kit (Bio-Rad, Hercules, CA). Quantitative PCR was performed on a CFX Connect thermal cycler (Bio-Rad) using iTaq Universal SYBR Green Supermix (Bio-Rad) and primers for three M-cell-associated genes. The relative expression of the M-cell-associated genes was determined by normalization to *Gapdh* using the comparative Ct method.

LGG culture and labeling. LGG provided by Dr Andrew Neish (Emory University) was grown overnight under anaerobic conditions with no shaking in MRS broth (BD Biosciences). To label the bacteria, 1×10^{10} washed bacteria were incubated in a total volume of 20 ml of phosphate-buffered saline (PBS) with 50 µg ml⁻¹ NHS-fluorescein (Thermo Fisher Scientific, Waltham, MA) for 30 min at 20 °C with constant agitation. The FITC-labeled bacteria were washed three times in PBS. Before gavage, the concentration of bacteria was determined using a Bacteria Counting Kit (Invitrogen) on a FACSCalibur flow cytometer (BD Biosciences).

Quantification of PP uptake of fluorescent bacteria or beads. Aliquots of 1×10^9 FITC-labeled LGG bacteria or 1×10^{11} 0.2-µm diameter polystyrene nanoparticles (Fluoresbrite YG; Polysciences, Warrington, PA) were administered by gavage to 6- to 8-week-old mice using a 20-gauge gavage needle in a total volume of 400 µl. Mice

given LGG bacteria were pretreated 5 min before gavage with 100 µl of 10% w/v sodium bicarbonate, to neutralize stomach acid. Multiple PPs were isolated either 6 h (LGG bacteria) or 24 h (nanoparticles) after gavage and snap frozen in optimal cutting temperature compound. Cryosections of PPs from mice administered nanoparticles were immediately counterstained with DAPI (5 µg ml⁻¹ in PBS). Cryosections of PPs from mice given FITC-labeled LGG bacteria were fixed for 20 min in acetone at -20 °C and mounted in 10 µl of ProLong Gold antifade reagent. The sections were imaged on a Nikon Eclipse 80i epifluorescence microscope to allow manual counting of uptake events.

Preparation of cell suspensions for flow cytometry. PPs and mesenteric lymph nodes were isolated and mechanically dissociated in ice-cold RPMI-1640 (Corning). The resulting cell suspensions were passed through a 70-µm mesh cell strainer. To prepare intestinal lamina propria cells, PPs were excised from the small intestine, the opened PP-free tissue was thoroughly washed in ice-cold PBS to remove luminal contents, and the small intestine was cut into 10 equal-sized pieces. The intestinal pieces were incubated for 15 min in PBS with 0.5 mM EDTA and 10 mM HEPES in a shaking incubator at 37 °C, and then strained through a large metal mesh strainer to remove epithelial cells. This step was repeated until no epithelial cells were visible in the supernatant. The intestinal fragments were washed thoroughly with PBS to remove the EDTA, minced exactly 30 times with a small scissors in a microfuge tube and incubated in 20 ml of RPMI-1640 supplemented with 10% fetal bovine serum, 0.25 mg ml⁻¹ Collagenase D (Roche, Indianapolis, IN), 0.25 mg ml⁻¹ Collagenase Fraction IV (MP Biomedicals, Santa Ana, CA), and 40 µg ml⁻¹ DNase I (Roche) for 20 min at 37 °C with constant agitation. After digestion, intestinal fragments were shaken vigorously by hand for 30 s and passed through a 100-µm mesh cell strainer. The cell suspension was sedimented at 1,000 g for 10 min and the resuspended pellet was further purified from the interface of a 30%/100% Percoll density gradient.

Flow cytometry analysis. The directly conjugated monoclonal antibodies used to stain cells for flow cytometry included PE-anti-mouse CD138 (281-2; BD Biosciences), FITC-anti-mouse IgA (C10-3; BD Biosciences), eFluor 450-anti-mouse IgD (11-25c; eBioscience), APC-anti-GL7 (GL7; eBioscience), FITC-anti-mouse PD-1 (294.1a12; BioLegend, San Diego, CA), PE-anti-mouse CXCR5 (L138D7; BioLegend), Brilliant Violet 605-anti-mouse B220 (RA3-6B2; BioLegend), PE-Cy7-anti-mouse CD19 (1D3; Tonbo Biosciences, San Diego, CA), APC-Cy7 anti-mouse CD45.2 (104; Tonbo Biosciences), and VF450-anti-mouse CD4 (RM4-5; Tonbo Biosciences). Live/dead cell discrimination for all antibody panels was done with Fixable Viability Dye eFluor 506 (eBioscience). Staining was carried out for 15 min at 20 °C in PBS with 1% bovine serum albumin and 0.02% NaN₃. After staining, all cells were fixed for 20 min at 20 °C in BD Fix/Perm buffer. To stain for intracellular IgA, cells were permeabilized for 20 min at 20 °C in BD Perm/Wash buffer and then stained for 15 min at 20 °C in BD Perm/Wash buffer. Stained cells were analyzed on an LSRII cytometer (BD Biosciences). Post-acquisition analysis of data files was done with FlowJo v9.3.1 software (Ashland, OR).

Processing of fecal pellets to yield fecal supernatant and fecal bacteria. Fresh fecal pellets were collected, weighed, and diluted 1:10 (w/v) in PBS with 1 mM EDTA. The suspension was vortexed for up to 15 min, to allow complete liquefaction, followed by centrifugation at 400 g at 4 °C for 5 min. The turbid supernatant was centrifuged a second time at 12,000 g for 10 min at 4 °C. The supernatant from this spin was used to determine the fecal IgA concentration by a sandwich enzyme-linked immunosorbent assay method using a IgA, κ-isotype control monoclonal antibody (BD Biosciences) as a standard, as previously described.²⁵ Fecal supernatants were stored at -80 °C after preparation and all supernatants from a single experiment were analyzed by enzyme-linked immunosorbent assay at the same time.

The concentration of IgA in serum samples was determined by the same enzyme-linked immunosorbent assay method. The remaining pellet containing fecal bacteria was fixed overnight in 4% paraformaldehyde. The fixed bacterial suspension was washed twice in PBS with 1% bovine serum albumin and 0.02% NaN₃, and stored in a 10% glycerol solution at -80°C until the bacteria were analyzed for bound IgA by flow cytometry.

Oral immunization with horse spleen ferritin. Five-week-old RANK^{ΔIEC} mice and RANK^{F/F} littermates were orally immunized with horse spleen ferritin (Sigma) using a modification of a previously described method.³⁰ Ferritin was added to the drinking water on days 0–2 and then again on days 7–9. Fecal samples were collected 2 weeks after the first day of immunization and were processed to prepare fecal supernatants by the same methods used to do measurements of total fecal IgA content. Serial dilutions of fecal supernatant from individual mice were tested for ferritin-specific fecal IgA by enzyme-linked immunosorbent assay using wells coated with ferritin. Bound anti-ferritin IgA antibody was detected with horseradish peroxidase-conjugated goat anti-mouse IgA (Southern Biotech, Birmingham, AL) followed by use of optEIA (BD Biosciences) as substrate.

Flow cytometric analysis of IgA bound to fecal bacteria. The density of fixed fecal bacteria in stored samples was estimated on the basis of OD₆₀₀. The equivalent of 1×10^6 live bacteria derived from a fresh *in vitro* culture was incubated in a solution containing 1 mg ml⁻¹ rat serum, 1.5% bovine serum albumin, and 0.5 μg ml⁻¹ of PE-anti-IgA (mAb-6E1; eBioscience) for 30 min at 20 °C in the dark. A PE-labeled rat IgG1 antibody (R3-34; BD Biosciences) was used as an isotype control. Bacterial suspensions were analyzed on an LSRII cytometer (BD Biosciences) using FSC-H and FSC-W to gate on bacterial events. The percentage of bacteria with bound IgA was determined using gates established by analysis of fecal bacteria from B-cell-deficient JH^{-/-} mice (Taconic) without any bound IgA.

Analysis of fecal microbiota composition by 16S sequencing. Fecal pellets from co-housed littermate RANK^{ΔIEC} and RANK^{F/F} mice were collected at 3, 7, 20, 30, and 40 days after weaning. DNA was extracted and amplified with forward 515F and reverse 806R primers flanking the V4 variable region as previously described.⁴⁴ Pooled products from four independent PCRs on each sample were purified and sequenced using an Illumina MiSeq sequencer. QIIME software was used to assign OTUs and perform rarefaction analysis.⁴⁵

Statistical analysis. Differences between the mean values for groups were analyzed by a two-tailed Student's *t*-test using Prism (GraphPad Software, La Jolla, CA). A *P*-value < 0.05 was considered significant.

SUPPLEMENTARY MATERIAL is linked to the online version of the paper at <http://www.nature.com/mi>

ACKNOWLEDGMENTS

We thank Dr Tim Denning for valuable suggestions and advice. We also thank Dr Lucie Etienne-Mesmin from the Gewirtz lab for assisting with husbandry of the germ-free RANK^{ΔIEC} mice and Dr Andrew Neish for providing the LGG bacterial strain. This work was supported by grants from the NIH (DK64730 to I.R.W., AI11388 to I.R.W. and A.T.G., and DK64399 supporting the Imaging Core Facility of the Emory Digestive Diseases Research Development Center) and the Crohn's & Colitis Foundation of America (Senior Research Award to I.R.W.). D.R. was supported in part by a Research Supplement to Promote Diversity in Health-Related Research from the NIH.

DISCLOSURE

The authors declare no conflict of interest.

REFERENCES

- Brandtzaeg, P. Secretory IgA: designed for anti-microbial defense. *Front. Immunol.* **4**, 222 (2013).
- Gutzeit, C., Magri, G. & Cerutti, A. Intestinal IgA production and its role in host-microbe interaction. *Immunol. Rev.* **260**, 76–85 (2014).
- Cebra, J.J., Periwai, S.B., Lee, G., Lee, F. & Shroff, K.E. Development and maintenance of the gut-associated lymphoid tissue (GALT): the roles of enteric bacteria and viruses. *Dev. Immunol.* **6**, 13–18 (1998).
- Macpherson, A.J., McCoy, K.D., Johansen, F.E. & Brandtzaeg, P. The immune geography of IgA induction and function. *Mucosal Immunol.* **1**, 11–22 (2008).
- Cerutti, A. The regulation of IgA class switching. *Nat. Rev. Immunol.* **8**, 421–434 (2008).
- Cao, A.T., Yao, S., Gong, B., Nurieva, R.I., Elson, C.O. & Cong, Y. Interleukin (IL)-21 promotes intestinal IgA response to microbiota. *Mucosal Immunol.* **8**, 1072–1082 (2015).
- Benckert, J. *et al.* The majority of intestinal IgA⁺ and IgG⁺ plasmablasts in the human gut are antigen-specific. *J. Clin. Invest.* **121**, 1946–1955 (2011).
- Peterson, D.A., McNulty, N.P., Guruge, J.L. & Gordon, J.I. IgA response to symbiotic bacteria as a mediator of gut homeostasis. *Cell Host Microbe* **2**, 328–339 (2007).
- Cullender, T.C. *et al.* Innate and adaptive immunity interact to quench microbiome flagellar motility in the gut. *Cell Host Microbe* **14**, 571–581 (2013).
- Bunker, J.J. *et al.* Innate and adaptive humoral responses coat distinct commensal bacteria with immunoglobulin A. *Immunity* **43**, 541–553 (2015).
- Palm, N.W. *et al.* Immunoglobulin A coating identifies colitogenic bacteria in inflammatory bowel disease. *Cell* **158**, 1000–1010 (2014).
- Shroff, K.E., Meslin, K. & Cebra, J.J. Commensal enteric bacteria engender a self-limiting humoral mucosal immune response while permanently colonizing the gut. *Infect. Immun.* **63**, 3904–3913 (1995).
- Macpherson, A.J., Gatto, D., Sainsbury, E., Harriman, G.R., Hengartner, H. & Zinkernagel, R.M. A primitive T cell-independent mechanism of intestinal mucosal IgA responses to commensal bacteria. *Science* **288**, 2222–2226 (2000).
- Schulz, O. & Pabst, O. Antigen sampling in the small intestine. *Trends Immunol.* **34**, 155–161 (2013).
- Mabbott, N.A., Donaldson, D.S., Ohno, H., Williams, I.R. & Mahajan, A. Microfold (M) cells: important immunosurveillance posts in the intestinal epithelium. *Mucosal Immunol.* **6**, 666–677 (2013).
- Rescigno, M. *et al.* Dendritic cells express tight junction proteins and penetrate gut epithelial monolayers to sample bacteria. *Nat. Immunol.* **2**, 361–367 (2001).
- Chieppa, M., Rescigno, M., Huang, A.Y. & Germain, R.N. Dynamic imaging of dendritic cell extension into the small bowel lumen in response to epithelial cell TLR engagement. *J. Exp. Med.* **203**, 2841–2852 (2006).
- Farache, J. *et al.* Luminal bacteria recruit CD103⁺ dendritic cells into the intestinal epithelium to sample bacterial antigens for presentation. *Immunity* **38**, 581–595 (2013).
- McDole, J.R. *et al.* Goblet cells deliver luminal antigen to CD103⁺ dendritic cells in the small intestine. *Nature* **483**, 345–349 (2012).
- Owen, R.L. & Jones, A.L. Epithelial cell specialization within human Peyer's patches: an ultrastructural study of intestinal lymphoid follicles. *Gastroenterology* **66**, 189–203 (1974).
- Neutra, M.R., Phillips, T.L., Mayer, E.L. & Fishkind, D.J. Transport of membrane-bound macromolecules by M cells in follicle-associated epithelium of rabbit Peyer's patch. *Cell Tissue Res.* **247**, 537–546 (1987).
- Bockman, D.E. & Cooper, M.D. Pinocytosis by epithelium associated with lymphoid follicles in the bursa of Fabricius, appendix, and Peyer's patches. An electron microscopic study. *Am. J. Anat.* **136**, 455–477 (1973).
- Owen, R.L. Sequential uptake of horseradish peroxidase by lymphoid follicle epithelium of Peyer's patches in the normal unobstructed mouse intestine: an ultrastructural study. *Gastroenterology* **72**, 440–451 (1977).
- Taylor, R.T. *et al.* Lymphotoxin-independent expression of TNF-related activation-induced cytokine by stromal cells in cryptopatches, isolated lymphoid follicles, and Peyer's patches. *J. Immunol.* **178**, 5659–5667 (2007).

25. Knoop, K.A. *et al.* RANKL is necessary and sufficient to initiate development of antigen-sampling M cells in the intestinal epithelium. *J. Immunol.* **183**, 5738–5747 (2009).
26. Dougall, W.C. *et al.* RANK is essential for osteoclast and lymph node development. *Genes Dev.* **13**, 2412–2424 (1999).
27. Hikosaka, Y. *et al.* The cytokine RANKL produced by positively selected thymocytes fosters medullary thymic epithelial cells that express auto-immune regulator. *Immunity* **29**, 438–450 (2008).
28. de Lau, W. *et al.* Peyer's patch M cells derived from Lgr5(+) stem cells require SpiB and are induced by RankL in cultured 'miniguts'. *Mol. Cell. Biol.* **32**, 3639–3647 (2012).
29. Kramer, D.R. & Cebra, J.J. Early appearance of 'natural' mucosal IgA responses and germinal centers in suckling mice developing in the absence of maternal antibodies. *J. Immunol.* **154**, 2051–2062 (1995).
30. Weisz-Carrington, P., Roux, M.E., McWilliams, M., Phillips-Quagliata, J.M. & Lamm, M.E. Organ and isotype distribution of plasma cells producing specific antibody after oral immunization: evidence for a generalized secretory immune system. *J. Immunol.* **123**, 1705–1708 (1979).
31. Benveniste, J., Lespinats, G. & Salomon, J. Serum and secretory IgA in axenic and holoxenic mice. *J. Immunol.* **107**, 1656–1662 (1971).
32. Crabbe, P.A., Bazin, H., Eyssen, H. & Heremans, J.F. The normal microbial flora as a major stimulus for proliferation of plasma cells synthesizing IgA in the gut. The germ-free intestinal tract. *Int. Arch. Allergy Appl. Immunol.* **34**, 362–375 (1968).
33. Mestecky, J. The common mucosal immune system and current strategies for induction of immune responses in external secretions. *J. Clin. Immunol.* **7**, 265–276 (1987).
34. Lindner, C. *et al.* Age, microbiota, and T cells shape diverse individual IgA repertoires in the intestine. *J. Exp. Med.* **209**, 365–377 (2012).
35. Bergqvist, P. *et al.* Re-utilization of germinal centers in multiple Peyer's patches results in highly synchronized, oligoclonal, and affinity-matured gut IgA responses. *Mucosal Immunol.* **6**, 122–135 (2013).
36. Hapfelmeier, S. *et al.* Reversible microbial colonization of germ-free mice reveals the dynamics of IgA immune responses. *Science* **328**, 1705–1709 (2010).
37. Yang, Q., Bermingham, N.A., Finegold, M.J. & Zoghbi, H.Y. Requirement of Math1 for secretory cell lineage commitment in the mouse intestine. *Science* **294**, 2155–2158 (2001).
38. Craig, S.W. & Cebra, J.J. Peyer's patches: an enriched source of precursors for IgA-producing immunocytes in the rabbit. *J. Exp. Med.* **134**, 188–200 (1971).
39. Mestecky, J., McGhee, J.R., Michalek, S.M., Arnold, R.R., Crago, S.S. & Babb, J.L. Concept of the local and common mucosal immune response. *Adv. Exp. Med. Biol.* **107**, 185–192 (1978).
40. Kunkel, E.J. & Butcher, E.C. Plasma-cell homing. *Nat. Rev. Immunol.* **3**, 822–829 (2003).
41. Brown, W.R. & Kloppel, T.M. The liver and IgA: immunological, cell biological and clinical implications. *Hepatology* **9**, 763–784 (1989).
42. Sato, T. & Clevers, H. Primary mouse small intestinal epithelial cell cultures. *Methods Mol. Biol.* **945**, 319–328 (2013).
43. Mahe, M.M. *et al.* Establishment of gastrointestinal epithelial organoids. *Curr. Protoc. Mouse Biol.* **3**, 217–240 (2013).
44. Chassaing, B., Ley, R.E. & Gewirtz, A.T. Intestinal epithelial cell toll-like receptor 5 regulates the intestinal microbiota to prevent low-grade inflammation and metabolic syndrome in mice. *Gastroenterology* **147**, 1363–1377 (2014).
45. Caporaso, J.G. *et al.* QIIME allows analysis of high-throughput community sequencing data. *Nat. Methods* **7**, 335–336 (2010).



This work is licensed under a Creative Commons Attribution-NonCommercial-ShareAlike 4.0 International License. The images or other third party material in this article are included in the article's Creative Commons license, unless indicated otherwise in the credit line; if the material is not included under the Creative Commons license, users will need to obtain permission from the license holder to reproduce the material. To view a copy of this license, visit <http://creativecommons.org/licenses/by-nc-sa/4.0/>